

RESPONSE SURFACE METHODOLOGY-AIDED DEVELOPMENT OF PIRFENIDONE-LOADED SOLID LIPID NANOPARTICLES FOR INTRAPULMONARY DRUG DELIVERY SYSTEM

KEVIN KWOK¹, GATOT SUHARIYONO², SILVIA SURINI^{1*}

¹Laboratory of Pharmaceutics and Pharmaceutical Technology, Faculty of Pharmacy, Universitas Indonesia, Depok, West Java-16424, Indonesia. ²Nuclear Metrology and Quality Safety Technology Research Center–Nuclear Power Research Organization, National Research and Innovation Agency, South Tangerang, Indonesia

*Corresponding author: Silvia Surini; *Email: silvia@farmasi.ui.ac.id

Received: 26 Dec 2023, Revised and Accepted: 01 May 2024

ABSTRACT

Objective: This study aims to determine the optimized Pirfenidone-loaded Solid Lipid Nanoparticles (P-SLN) formula for Intrapulmonary Drug Delivery System (IPDDS) using Response Surface Methodology (RSM).

Methods: Box-Behnken design was applied to create fifteen P-SLN formulas comprising three independent variables, namely lipid-to-drug ratio, polymer type, and polymer concentration, and three dependent variables, including particle size, Polydispersity Index (PDI), and entrapment efficiency. The P-SLNs were prepared by solvent injection followed by the ultrasonication method. Those formulas were optimized with the RSM approach using the Design Expert®. Then, the optimized P-SLN was further characterized for morphology, moisture content, aerodynamic performance, and dissolution profile.

Results: The optimization process, assisted by RSM, determined that the optimized P-SLN had a lipid-to-drug ratio of 6:1 and contained 0.5% Plasdone K-29/32. The resulting P-SLN had a spherical shape with a particle size of 212.7 nm, a PDI of 0.39, an entrapment efficiency of 95.02%, and a low moisture content of 1.59%. The optimized P-SLN also exhibited appropriate IPDDS required characteristics, including a Mass Median Aerodynamic Diameter (MMAD) ranging from 0.540–12.122 μm and a Respirable Fraction (RF) of 12.4%. Moreover, the release of pirfenidone from this optimized formula was 89.61% and 69.28% in pH 4.5 and 7.4 buffer media, respectively, in 45 min through a combination of diffusion and polymer swelling mechanisms.

Conclusion: The optimized P-SLN showed promising potential as an IPDDS for pirfenidone.

Keywords: Pirfenidone, Lipid nanoparticles, Formula optimization, Mass median aerodynamic diameter, Box-Behnken design

© 2024 The Authors. Published by Innovare Academic Sciences Pvt Ltd. This is an open access article under the CC BY license (<https://creativecommons.org/licenses/by/4.0/>) DOI: <https://dx.doi.org/10.22159/ijap.2024v16i4.50231> Journal homepage: <https://innovareacademics.in/journals/index.php/ijap>

INTRODUCTION

Pirfenidone, a hydrophobic antifibrotic drug, is used in Pulmonary Fibrosis (PF) treatment [1]. PF is a progressive and chronic lung disease that could cause stiffness of the alveoli, reduce oxygen-CO₂ diffusion, and disrupt the respiratory process [2]. A cohort study on COVID-19 survivors in China concluded that about 56% of the survivors exhibited a reduction in lung function and tissue disruption similar to PF symptoms [3]. Pirfenidone has been studied in clinical trials to treat COVID-19 survivors who developed PF, and the results showed an improvement in total lung capacity and oxygen-CO₂ diffusion. Furthermore, the chest Computed Tomography (CT) scan performed on the survivors after two years of PF illness showed a fibrosis reduction [4].

In current PF treatment, pirfenidone is administered through the peroral route. However, orally administered pirfenidone undergoes first-pass metabolism into its inactive form, necessitating high dose levels (up to 2,403 mg/d) and increasing systemic adverse effects, particularly skin phototoxic reaction [5]. Consequently, research has been conducted to develop an alternative route for pirfenidone administration. Intrapulmonary Drug Delivery System (IPDDS) might be an alternative route to deliver pirfenidone locally in the lungs, thus avoiding the first-pass metabolism and reducing the systemic adverse effect [6].

As PF-scarred tissues are found in the alveolar regions, developing an IPDDS that can reach and deposit at certain deep lung regions is crucial. The particles in an IPDDS must be smaller than 500 nm to target the alveoli, and this characteristic is derived from nanoparticles [7]. In this context, Solid Lipid Nanoparticles (SLN), which are capable of encapsulating hydrophobic drugs and depositing the particles in the alveolar region through the Brownian diffusion mechanism, might become a potential carrier for pirfenidone [8]. Furthermore, SLN can minimize the mobility of the entrapped drugs with its solid lipid structure. Hence, the expulsion

of the entrapped drug from the nanoparticle carrier could be diminished [9].

In general, two major parameters have a significant impact on SLN characteristics. The first is the formulation parameter, such as lipid type, total lipid concentration, lipid-to-drug ratio, surfactant or stabilizing polymer type, stabilizer concentration, etc. The second is the process parameters, which depend on the SLN production method. In this study, the SLN was produced by solvent injection followed by the ultrasonication method, which has been optimized from previous study [10]. Hence, the parameter processes such as temperature, homogenization rate, homogenization duration, sonication energy, and sonication duration were kept constant [11]. Therefore, the SLN formulation parameter should be optimized to achieve SLN with optimum characteristics. Previous research reported that the lipid-to-drug ratio could affect the particle size and Polydispersity Index (PDI) of the produced SLN [12]. Meanwhile, the type and concentration of stabilizing polymers could affect the particle size and entrapment efficiency of the SLN [13]. Based on this information, we selected the lipid-to-drug ratio, type of polymer, and polymer concentration as the factors in the optimization process. However, optimizing these multiple factors separately regarding the required time and number of experiments would be inefficient and complicated. Thus, a more efficient approach, namely Response Surface Methodology (RSM), is required to optimize multiple factors simultaneously.

In recent years, RSM has captured the interest of researchers worldwide who perform optimization studies due to its advantages, such as being capable of optimizing multiple factors simultaneously, assisting in designing experiments, providing statistical analysis, and accounting for the interactions between factors in the optimization process. Moreover, RSM also aids the users in predicting optimum responses [14, 15]. This study aimed to achieve the optimized Pirfenidone-loaded Solid Lipid Nanoparticles (P-SLN) formula with

ideal characteristics for IPDDS using RSM. Fifteen P-SLN formulas of were prepared based on the Box-Behnken Design (BBD) by varying lipid-to-drug ratio, type of polymer, and polymer concentration. The Particle Size (PS), PDI, and Entrapment Efficiency (EE) of the P-SLN were statistically analyzed and optimized using Design Expert®. Additionally, the morphology, moisture content, aerodynamic performance, and *in vitro* dissolution profiles of the optimized P-SLN were characterized.

MATERIALS AND METHODS

Materials

Pirfenidone was purchased from Accela Chembio (Shanghai, China), Glycerol Monostearate (GMS) was purchased from Spectrum (New Jersey, USA), Tween 80 was acquired from Gracefruit Ltd. (Bonnybridge, United Kingdom), poloxamer 188, methanol, ethanol,

and acetonitrile were purchased from Merck (Darmstadt, Germany). Plasdane K-29/32 and Klucel LF were generously provided by Ashland Pharmaceuticals (Wilmington, USA).

Experimental design

BBD was applied to create 15 different formulations based on three independent variables, namely lipid-to-drug ratio (X_1), polymer type (X_2), and polymer concentration (X_3). The polymers used were poloxamer 188, Plasdane K-29/32, and Klucel LF, encoded as 1, 2, and 3, respectively. The assessed responses were PS (Y_1), PDI (Y_2), and EE (Y_3), while the levels of the factor, constraints, and goals for each response are presented in Table 1. Design Expert® software (version 13, Stat-ease Inc., USA) was used for the optimized P-SLN formula, comprising steps such as regression model selection, ANOVA analysis, polynomial equation generation, surface response modeling, optimum formula prediction, and confirmation.

Table 1: Factors and responses of the optimized P-SLN formula

Factors	Level			Responses	Constraints	Goals
	-1	0	+1			
Lipid-to-drug ratio (X_1)	5	10	15	PS (Y_1)	100–300 nm	Minimum
Type of polymer (X_2)	1	2	3	PDI (Y_2)	<0.5	Minimum
Polymer concentration (%) (X_3)	0.5	1	1.5	EE (Y_3)	>90%	Maximum

PS = Particle Size, PDI = Polydispersity Index, EE = Entrapment Efficiency

Preparation of P-SLN

P-SLN was prepared using solvent injection followed by ultrasonication method, where 0.2 g of pirfenidone and a particular amount of GMS were dissolved in 6 ml pre-heated ethanol at 55°C (organic phase). Simultaneously, 1g of Tween 80 and the selected polymer were dissolved in 100 ml pre-heated distilled water at 55 °C (aqueous phase). The organic phase was slowly added to the aqueous phase and homogenized at 10,000 rpm under 55 °C temperature for 15 min (Ultraturrax® T-25 Easy Clean, IKA, Germany). The resulting dispersion was then subjected to a probe sonicator (Qsonica®Cl-334, USA) at 55% amplitude for 10 min (on for 3 seconds and off for 2 seconds). After cooling to room temperature, SLN solidified, and its suspension was stored in a freezer overnight at -20 °C and lyophilized for 24 h.

Particle size and polydispersity index measurements of P-SLN

A 10 mg lyophilized P-SLN was dispersed in 10 ml distilled water and then diluted tenfold. PS and PDI of the diluted P-SLN dispersion were determined using Zetasizer Nano ZS-90 (Malvern Instrument Ltd., United Kingdom) at 25 °C with a scattering angle of 90°.

Entrapment efficiency determination of P-SLN

EE was determined using the direct method with HPLC (Shimadzu SPD-20A, Japan). A mobile phase consisting of acetonitrile and water (65:35, v/v) was pumped at a flow rate of 0.7 ml/min through a C_{18} column (4.6 × 250 mm, 5 μm) (Zorbax Eclipse Plus, Agilent, USA). Lyophilized P-SLN, equivalent to 2.5 mg pirfenidone, was accurately weighed, dissolved in 25 ml methanol, and then sonicated for 20 min. A 0.6 ml aliquot was diluted with the mobile phase to reach a final volume of 10 ml. The solution was filtered through a 0.45 μm PTFE filter and analyzed at 317 nm [16]. Entrapment efficiency percentage was calculated using the following equation:

$$EE (\%) = \frac{\text{Actual amount of PFD in lyophilized P - SLN (mg)}}{\text{The theoretical amount of PFD in formulation (mg)}} \times 100\%$$

Optimization of P-SLN formula

The collected responses were analyzed using Design Expert 13.0 software by fitting the responses to several mathematical models and comparing the obtained R^2 values. The model with the highest R^2 value was selected for further analysis. ANOVA was used to assess the significance of the effects of factors on responses. Moreover, the software automatically generated three-dimensional surface plots and polynomial equations. The optimum predicted formula with the highest desirability was confirmed through experiments.

Moisture content measurement

Approximately 0.5 g lyophilized P-SLN was accurately weighed and then subjected to a moisture balance analyzer for the moisture content (% w/w) measurement.

Particle morphology identification

The morphology of P-SLN was observed with Transmission Electron Microscopy (TEM) (Jeol JEM 1400, USA). A total of 10 mg lyophilized P-SLN was dispersed in 10 ml distilled water. One drop of this dispersion was placed onto a carbon-coated copper grid, and a 2% phosphotungstic acid solution was added. Subsequently, the sample was observed under TEM at various magnifications.

Aerodynamic performance study

The aerodynamic performance study was conducted using the Anderson Cascade Impactor. Approximately 250 mg lyophilized P-SLN was aerosolized at a flow rate of 28.3 L/min for 4 min. The mass of deposited particles at each stage was weighed and inputted to the impactor data processing software to obtain the Mass Median Aerodynamic Diameter (MMAD) [17]. The Respirable Fraction (RF) was calculated using the following equation:

$$RF (\%) = \frac{\text{Amount of lyophilized P - SLN with size below } 5 \mu\text{m (mg)}}{\text{Amount of loaded lyophilized P - SLN (mg)}} \times 100\%$$

In vitro dissolution and drug release study

The dissolution study was performed through the dialysis bag technique using two different media: Pulmonary Simulation Fluid (PSF) and Pulmonary Macrophage Simulation Fluid (PMSF). PSF was prepared from Phosphate Buffer Saline (PBS) at pH 7.4, containing 0.05% sodium lauryl sulfate, while PMSF was produced from 0.02 M potassium hydrogen phthalate at pH 4.5 [18]. Lyophilized P-SLN equivalent to 6 mg pirfenidone was dispersed in 5 ml aquadest and filled into pre-hydrated dialysis bags (molecular weight cut-off 12–14 kDa). The bags were placed inside a 50 ml pre-heated medium at 37 °C and stirred at 100 rpm. Samples of 1 ml were collected for HPLC analysis and replaced with 1 ml fresh medium at 5, 10, 15, 20, 30, and 45 min [17]. The drug release mechanism was determined by fitting the dissolution data from tested samples into several kinetic model equations.

RESULTS

Characterization of P-SLN

The evaluated factors and their respective effects on each response are presented in Table 2. The particle size of the produced P-SLN was within the required particle size for IPDDS, ranging from 193.7

to 295.7 nm. Formula F1, with a lipid-to-drug ratio of 5:1 and 1% poloxamer 188, had the lowest average PS (193.7 nm). In

comparison, formula F11 consists of a lipid-to-drug ratio of 10:1, and 0.5% Klucel LF had the largest average PS (295.7 nm).

Table 2: Effect of formulation on P-SLN characteristics based on Box-Behnken design

Formula	Lipid-to-drug ratio (X_1)	Type of polymer (X_2)	Polymer concentration (%), (X_3)	PS (nm) (Y_1)	PDI (Y_2)	EE (%) (Y_3)
F1	5	1	1	193.7±5.0	0.57±0.14	63.71±3.71
F2	5	3	1	265.7±11.9	0.36±0.02	65.60±4.36
F3	15	1	1	271.7±6.3	0.47±0.03	72.70±2.66
F4	15	3	1	211.2±11.2	0.57±0.18	68.77±2.82
F5	5	2	0.5	225.7±11.8	0.35±0.02	91.59±3.74
F6	5	2	1.5	234.2±15.8	0.41±0.01	84.57±2.26
F7	15	2	0.5	231.7±18.7	0.40±0.10	94.50±2.24
F8	15	2	1.5	249.4±5.0	0.38±0.06	93.07±2.90
F9	10	1	0.5	239.6±13.6	0.46±0.07	93.20±2.36
F10	10	1	1.5	286.5±18.7	0.80±0.08	89.77±2.30
F11	10	3	0.5	295.7±7.2	0.73±0.09	91.97±3.82
F12	10	3	1.5	258.9±12.1	0.43±0.04	87.21±2.53
F13	10	2	1	209.6±6.0	0.50±0.08	93.20±1.36
F14	10	2	1	203.2±20.2	0.50±0.15	93.39±1.25
F15	10	2	1	206.4±24.4	0.51±0.06	93.31±0.10

PS = Particle Size, PDI = Polydispersity Index, EE = Entrapment Efficiency. All values are presented as mean±standard deviation (n = 3)

Table 2 also showed the PDI results of the produced P-SLN. It can be observed that the PDI ranged from 0.35 to 0.80. The lower PDI value (less than 0.5) indicated a narrower size distribution, and the more homogenous particles would be obtained. The lowest PDI was obtained from formula F5, which consists of a lipid-to-drug ratio of 5:1 and 0.5% plasdone K-29/32.

According to Table 2, the EE of the obtained P-SLN ranged from 63.71 to 94.50%. Based on the characterization results, it can be observed that formulas with plasdone K-29/32 (F5, F7, F8, F13, F14, and F15) were found to had EE more than 90%, with the highest value of 94.50% from formula F7.

Formula optimization of P-SLN

The characterization results collected from fifteen P-SLN formulas were input to Design Expert®. Then, linear, two-factor interaction, and quadratic models were used to analyze the best model from the input data. The best model was selected based on the p-value of the model and lack of fit. Models should be significant ($p < 0.05$), while lack of fit should be insignificant ($p > 0.05$). According to the model fit analysis, the influence of all factors on each response was assessed through the quadratic model, which indicated a non-linear correlation between factors and responses. The polynomial equations are presented in Table 3, while the three-dimensional response surface plots are depicted in 1.

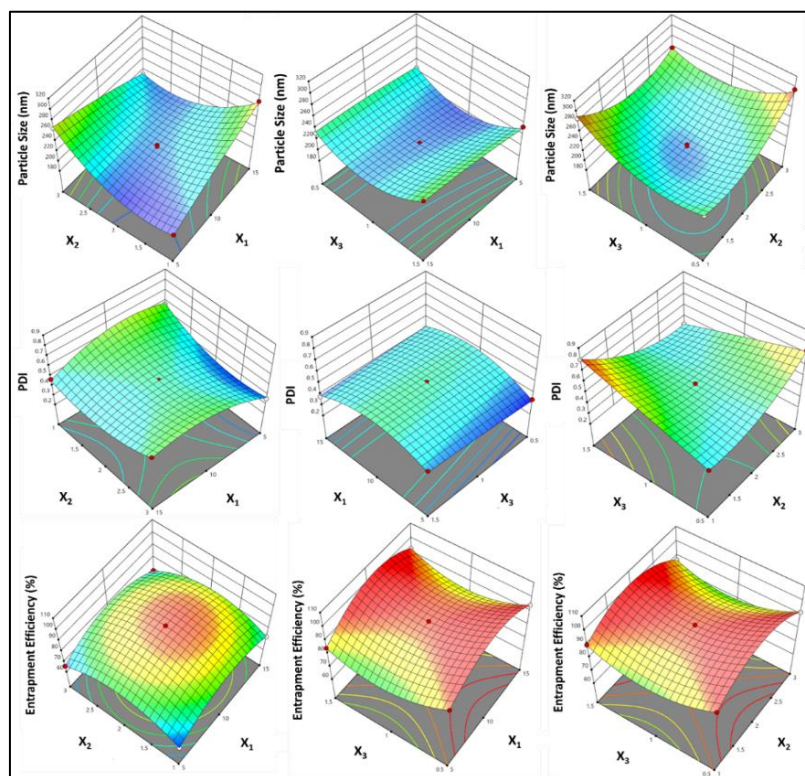


Fig. 1: Three-dimensional response surface plots of P-SLN based on PS (top), PDI (middle), and EE (bottom). The factors are X_1 = ratio of lipid-to-drug; X_2 = type of polymer (1. Poloxamer 188, 2. Pladone K-29/32, and 3. Klucel LF); X_3 = Polymer concentration (%)

Table 3: Polynomial equations for each response

Response	Polynomial equation
PS (Y_1)	$Y_1 = -2.89X_1^2 + 32.06X_2^2 + 31.71X_3^2 - 33.13X_1X_2 + 2.33X_1X_3 - 20.93X_2X_3 + 5.58X_1 + 5.00X_2 + 4.55X_3 + 206.40$
PDI (Y_2)	$Y_2 = -0.005X_1^2 + 0.105X_2^2 - 0.012X_3^2 + 0.016X_1X_2 - 0.010X_1X_3 - 0.320X_2X_3 + 0.074X_1 - 0.280X_2 + 0.788X_3 + 0.013$
EE (Y_3)	$Y_3 = -0.50X_1^2 - 13.00X_2^2 + 40.95X_3^2 - 0.29X_1X_2 + 0.56X_1X_3 - 0.67X_2X_3 + 10.70X_1 + 54.85X_2 - 90.32X_3 + 30.00$

X_1 = lipid-to-drug ratio, X_2 = type of polymer, X_3 = polymer concentration, PS = Particle Size, PDI = Polydispersity Index, EE = Entrapment Efficiency

The formula optimization process was performed using Design Expert® by overlaying all nine three-dimensional response surface plots. The response variables were optimized based on predefined

constraints and goals in Table 1. This process generated a design space, visually represented in an overlay plot (2), aiding the identification and prediction of the optimum region.

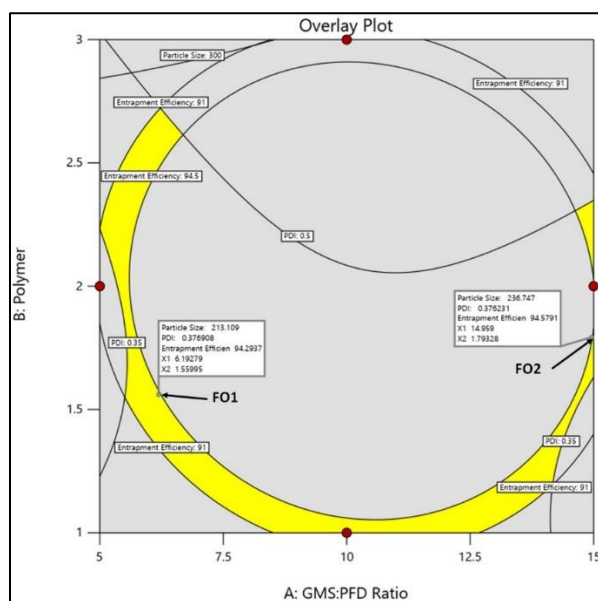


Fig. 2: Overlay plot of the predicted optimized formula

Confirmation of optimum predicted formula

The optimum predicted formula was selected based on the highest desirability value. Design Expert software predicted two optimized formulas, FO1 and FO2, which had lipid-to-drug ratios of 6:1 and 15:1, each with 0.5% Pladone K-29/32 and desirability values of 0.900 and 0.813, respectively. The predicted particle size, PDI, and efficiency values for FO1 and

FO2 were obtained from the software and are presented in Table 4. Then, both formulas were confirmed through experiment. The response values obtained from the experiments were denoted as the actual value and were also presented in Table 4. Furthermore, the residual error between predicted and actual values was calculated to validate the confirmation results. The calculated residual error of PS, PDI, and EE for FO1 and FO2 was less than 10%, as indicated in Table 4.

Table 4: Confirmation results of the optimized P-SLN based on RSM

Formula	Factors			Response	Predicted value	Actual value	Residual error (%)
	X_1	X_2	X_3				
FO1	6	2	0.5	PS (nm)	213.1	212.7	0.19
				PDI	0.38	0.39	2.63
				EE (%)	94.29	95.02	0.77
FO2	15	2	0.5	PS (nm)	236.8	234.7	0.89
				PDI	0.38	0.39	2.63
				EE (%)	94.58	95.04	0.49

X_1 = lipid-to-drug ratio, X_2 = type of polymer, X_3 = polymer concentration, PS = particle size, PDI = polydispersity index, EE = entrapment efficiency

Morphological examination of the optimized P-SLN

Morphological examination on optimized P-SLN was conducted using a TEM at various magnifications. The results showed that particles from the optimized P-SLN formulas exhibited a spherical shape, as indicated in 3.

Moisture content and aerodynamic performance of the optimized P-SLN

According to Table 5, FO2, with a greater amount of GMS, had a higher moisture content than FO1. Aerodynamic performance characterization showed that FO1 and FO2 had a Geometric Standard Deviation (GSD) of more than 1.22, indicating a multimodal distribution for P-SLN particles [19]. This characteristic would affect deposited particle distribution in the respiratory tract. Based on data

analysis, FO1 exhibited MMAD ranging from 0.540–12.122 μm and approximately 78.58%, 17.86%, and 3.56% of FO1 particles possessed MMAD of more than 6 μm , 1–5 μm , and less than 1 μm , respectively. Meanwhile, FO2 exhibited MMAD ranging from 0.710–13.490 μm , with

92.96%, 5.26%, and 1.78% of particles possessed MMAD of more than 6 μm , 1–5 μm , and less than 1 μm , respectively. Table 5 also presents the RF of FO1 and FO2. The results showed that both optimized P-SLN had low RF. However, FO2 exhibited a lower RF than FO1.

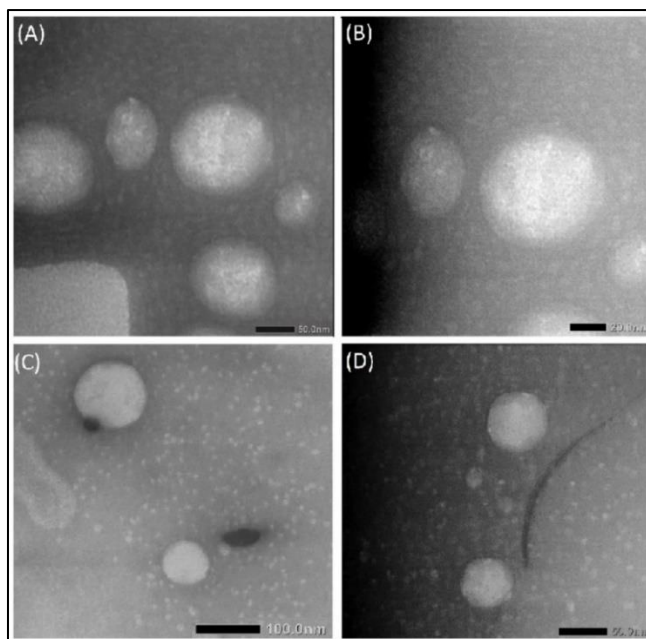


Fig. 3: TEM micrographs of optimized P-SLN based on FO1 with 80,000 \times magnification (A) and 150,000 \times magnification (B) and FO2 with 40,000 \times magnification (C) and 80,000 \times magnification (D)

Table 5: Characteristics of FO1 and FO2

Formula	Characteristics				
	Moisture content* (%)	MMAD (μm)	GSD	Mass distribution (%)	RF (%)
FO1	1.59 \pm 0.09	0.540	1.845	3.56	12.4
		1.304	1.487	17.86	
		5.531	1.268	23.82	
		12.122	1.264	54.75	
FO2	2.71 \pm 0.12	0.710	1.259	1.78	10.4
		2.311	1.259	5.26	
		5.362	1.259	22.11	
		13.490	1.259	70.85	

MMAD = Mass Median Aerodynamic Diameter, GSD = Geometric Standard Deviation, RF = Respirable Fraction. *values presented as mean \pm SD (n=3)

***In vitro* dissolution and kinetic release study of the optimized formula**

The dissolution study of FO1 and FO2 was conducted in two types of dissolution media, and the dissolution profiles are presented in 4. The release rate of pirfenidone from FO1 was significantly faster than FO2 in both media ($p < 0.05$). The results also showed that

pirfenidone was released significantly faster in PMSF at pH 4.5 than in PSF at pH 7.4 ($p < 0.05$). This discrepancy was attributed to the higher solubility of pirfenidone in PMSF (± 20.0 mg/ml) compared to PSF (± 19.3 mg/ml). According to previous research, GMS had better solubility properties in acidic media than in basic ones, further accelerating the release of pirfenidone from the P-SLN system in PMSF at pH 4.5 [20].

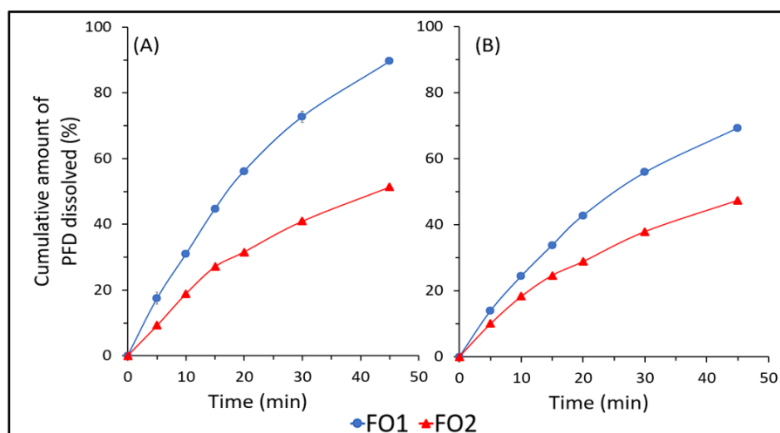


Fig. 4: Pirfenidone dissolution profile of FO1 (♂) and FO2 (♀) in PMSF pH 4.5 (A) and PSF pH 7.4 (B). All values are presented as mean±SD (n=3)

The kinetics of pirfenidone release from FO1 and FO2 were determined by calculating the *r* value for several kinetic models. The results showed that the Korsmeyer-Peppas model had the

highest correlation coefficient values with an *n* coefficient of about 0.70–0.77 for both formulas in the two-dissolution media (Table 6).

Table 6: Drug release kinetics of FO1 and FO2

Formula	Zero-order		First order		Higuchi		Korsmeyer-Peppas		
	k (min ⁻¹)	r	k (min ⁻¹)	r	k (min ^{-1/2})	r	k (min ⁻¹)	r	n
PMSF pH 4.5									
FO1	0.020	0.977	0.037	0.913	0.140	0.986	0.054	0.995	0.76
FO2	0.011	0.974	0.037	0.893	0.080	0.987	0.030	0.989	0.77
PSF pH 7.4									
FO1	0.015	0.979	0.037	0.921	0.108	0.987	0.044	0.997	0.74
FO2	0.010	0.974	0.034	0.916	0.073	0.992	0.035	0.995	0.70

k = Release rate constant, r = correlation coefficient, n = release mechanism exponent, PMSF = Pulmonary Macrophage Simulation Fluid, PSF = Pulmonary Simulation Fluid

DISCUSSION

In this study, we optimized the P-SLN formula comprising lipid-to-drug ratio, type of polymer, and polymer concentration. PS, PDI, and EE were selected as the critical responses during the optimization. Our characterization results from fifteen P-SLN formulas showed that lipid-to-drug ratio, type of polymer, and polymer concentration affect all responses. Thus, our characterization results confirmed the results from previous studies [12, 13, 21]. The polynomial equation and three-dimensional response surface plots (Table 3 and 1) derived from Design Expert® software showed that the factors had a non-linear correlation toward the responses. This result indicated that the interaction between factors existed, and the responses could be influenced by the interaction between factors as well as each factor individually. Consequently, explaining the correlation between factors and the obtained responses would be difficult.

The optimization process was performed by overlaying all response surface plots. It produced two optimum predicted formulas with lipid-to-drug ratios of 6:1 and 15:1, each with 0.5% Plasdone K-29/32, as well as desirability values of 0.900 and 0.813, denoted as FO1 and FO2, respectively. The confirmation results showed that the calculated residual error of PS, PDI, and EE for both optimized formulas was less than 10%. It indicates a high agreement between the actual responses and predicted values, validating the optimization results [22]. Since FO1 with lower lipid content produced P-SLN characteristics that are not significantly different from FO2, FO1 is suggested as the preferable formula.

Morphological examination showed that both optimized formulas had a spherical shape. Spherical particles were observed to produce a better aerodynamic performance than non-spherical counterparts. This was due to the lower mechanical interlocking interaction of spherical particles, enhancing the fluidization properties in the airstream [23]. As Table 5 shows, FO2 had a higher moisture content than FO1. A high moisture content may decrease the fluidization

properties of the particles in the airstream due to the stickiness properties, thus increasing the aerodynamic particle size [24].

Results from the aerodynamic performance study showed that FO1 exhibited MMAD ranging from 0.540– 2.22 μm and approximately 78.58%, 17.86%, and 3.56% of FO1 particles possessed MMAD of > 6 μm, 1–5 μm, and < 1 μm, respectively. This distribution suggested the possibility of about 78.58%, 17.86%, and 3.56% of FO1 particles depositing in the oropharyngeal, bronchiolar, and alveolar regions due to inertial impaction, gravitational sedimentation, as well as Brownian diffusion mechanisms, respectively [25]. Meanwhile, FO2 exhibited MMAD ranging from 0.710–13.490 μm, with 92.96%, 5.26%, and 1.78% of particles tending to deposit in the oropharyngeal, bronchial, and alveolar regions. The results showed that FO2 exhibited a larger and broader MMAD distribution than FO1. This could be attributed to the higher moisture content of FO2, which led to particle aggregation.

MMAD, besides the deposition profile, determined the probability of particle phagocytosis by alveolar macrophages. A previous study reported that particles with MMAD greater than 1 μm were more liable to be engulfed [26]. Based on the current results, FO2 had approximately 98.22% of particles with MMAD exceeding 1 μm, while FO1 contained only 96.44%. This indicated that FO1 could comprise more particles capable of avoiding phagocytosis than FO2, signifying better aerodynamic performance for FO1.

Table 5 also presents the RF of FO1 and FO2. Our results showed that both optimized P-SLNs had low RF. Nevertheless, FO2 exhibited a lower RF than FO1. This could be attributed to the higher moisture content of FO2, which led to greater MMAD due to particle aggregation, reducing the RF of FO2. Previous research with similar results reported that the RF of most carrier-based IPDDS formulations is relatively low, with approximately only 10% of the total dose being delivered to the lower airways [27]. For future research, we suggest to improve the RF in order to enhance the efficiency of the P-SLN for IPDDS. Nevertheless, based on

our results, FO1 is suggested to be the best formula that has the most appropriate characteristics for IPDDS.

The dissolution profiles presented in 4 showed an initial burst release of PFD from FO1 and FO2 in both media, which could be due to the presence of the adsorbed drug on the surface of the SLN system. Another study reported a similar result, suggesting that this initial burst release might help provide the required pirfenidone concentration in the lungs [28]. The release rate of pirfenidone from FO1 was significantly faster than FO2 in both dissolution media. This difference was due to the higher amount of GMS in FO2, leading to a higher affinity of pirfenidone to GMS, decreasing the release rate [29]. A previous study reported that pirfenidone-loaded liposomes release up to 50% pirfenidone in PSF at pH 7.4 over 4 h [30]. In contrast, our results showed a faster pirfenidone release from P-SLN, reaching 50.5% in 45 min. The accelerated release might be due to the presence of Plasdome K-29/32, which could increase the hydration rate and porosity of the GMS matrix, enabling the dissolution medium to penetrate the matrix and rapidly form pores similar to pathways. This would subsequently enhance the diffusion of pirfenidone through the formed pores [31].

Table 6 presents the results of pirfenidone release from FO1 and FO2 in both dissolution media based on several kinetic models. Our results revealed that both optimized P-SLN formulas had the highest correlation coefficient values (r) in the Korsmeyer-Peppas model with an n coefficient of about 0.70–0.77 in both dissolution media. These indicated pirfenidone to be released from optimized P-SLN through a non-fickian diffusion, which is a combination of diffusion and polymer swelling mechanisms in both media [32].

The optimized P-SLN is prospected to be applied in treating PF through intrapulmonary administration. Previous study showed that rapid drug release would provide high drug concentrations locally in lung tissue [33]. Therefore, FO1 was considered the best among both optimized formulas as it could rapidly release pirfenidone and achieve higher pirfenidone concentrations in both dissolution media. Further investigation in *in vivo* studies should be conducted to assess the effectiveness of the P-SLN through the intrapulmonary route compared to the peroral pirfenidone.

CONCLUSION

In conclusion, the application of RSM in this study successfully yielded two optimized P-SLN formulas. However, FO1 showed superiority over FO2 due to the ability to achieve comparable P-SLN characteristics with less lipid content. FO1, comprising a 6:1 lipid-to-drug ratio and 0.5% Plasdome K-29/32, produced spherical P-SLN with a PS of 212.7 nm, PDI of 0.39, EE of 95.02%, and low moisture content of 1.59%. In addition, it exhibited suitable aerodynamic performance for IPDDS, with MMAD ranging from 0.540–12.122 μ m and RF of 12.4%. The dissolution study indicated that pirfenidone release from FO1 reached 89.61% and 69.28% in PMSF at pH 4.5 and PSF at pH 7.4, respectively, over 45 min, primarily through a combination of diffusion and polymer swelling mechanisms. Our results suggested FO1 as a potential candidate for IPDDS and should be further investigated for efficacy in *in vivo* studies.

ACKNOWLEDGMENT

The authors are thankful to Universitas Indonesia, Depok, Indonesia and National Research and Innovation Agency, Jakarta, Indonesia for providing necessary facilities to conduct the research. The authors are also thankful to Ashland Pharmaceuticals for providing the required materials for this research.

FUNDING

Nil

AUTHORS CONTRIBUTIONS

Kevin Kwok contributed to designing the experiment, acquiring, analyzing and interpreting data, and preparing and editing manuscript. Silvia Surini made a significant contribution in designing the experiment, analyzing and interpreting data, and reviewing the manuscript as the final guarantor. Gatot Suhariyono

contributed to data analysis, data interpretation, and manuscript review.

CONFLICTS OF INTERESTS

The authors report that there are no conflicts of interest regarding the publication of this article

REFERENCES

- Ruwanpura SM, Thomas BJ, Bardin PG. Pirfenidone: molecular mechanisms and potential clinical applications in lung disease. *Am J Respir Cell Mol Biol.* 2020;62(4):413-22. doi: 10.1165/rcmb.2019-0328TR, PMID 31967851.
- Martinez FJ, Collard HR, Pardo A, Raghu G, Richeldi L, Selman M. Idiopathic pulmonary fibrosis. *Nat Rev Dis Primers.* 2017;3(17074):17074. doi: 10.1038/nrdp.2017.74, PMID 29052582.
- Huang C, Huang L, Wang Y, Li X, Ren L, Gu X. 6 mo consequences of COVID-19 in patients discharged from hospital: a cohort study. *Lancet.* 2021;397(10270):220-32. doi: 10.1016/S0140-6736(20)32656-8, PMID 33428867.
- Zhou X, Yang D, Kong X, Wei C, LvQiu S, Wang L. Case report: pirfenidone in the treatment of post-COVID-19 pulmonary fibrosis. *Front Med (Lausanne).* 2022;9:(925703). doi: 10.3389/fmed.2022.925703, PMID 35733875.
- Seto Y, Inoue R, Kato M, Yamada S, Onoue S. Photosafety assessments on pirfenidone: photochemical, photobiological, and pharmacokinetic characterization. *J Photochem Photobiol B.* 2013;120:44-51. doi: 10.1016/j.jphotobiol.2013.01.010, PMID 23419534.
- Park JH, Jin HE, Kim DD, Chung SJ, Shim WS, Shim CK. Chitosan microspheres as an alveolar macrophage delivery system of ofloxacin via pulmonary inhalation. *Int J Pharm.* 2013;441(1-2):562-9. doi: 10.1016/j.ijpharm.2012.10.044, PMID 23142421.
- Gulati N, Chellappan DK, MacLoughlin R, Dua K, Dureja H. Inhaled nano-based therapeutics for inflammatory lung diseases: recent advances and future prospects. *Life Sci.* 2021;285:(119969). doi: 10.1016/j.lfs.2021.119969, PMID 34547339.
- Abdelaziz HM, Gaber M, Abd-Elwakil MM, Mabrouk MT, Elgohary MM, Kamel NM. Inhalable particulate drug delivery systems for lung cancer therapy: nanoparticles, microparticles, nanocomposites and nanoaggregates. *J Control Release.* 2018;269:374-92. doi: 10.1016/j.jconrel.2017.11.036, PMID 29180168.
- Duan Y, Dhar A, Patel C, Khimani M, Neogi S, Sharma P. A brief review on solid lipid nanoparticles: part and parcel of contemporary drug delivery systems. *RSC Adv.* 2020;10(45):26777-91. doi: 10.1039/d0ra03491f, PMID 35515778.
- Anggraini R, Surini S, Saputri FC. Formulation and characterization of bitter melon (*Momordica charantia* linn.) fruit fraction loaded solid lipid nanoparticles. *Pharmacogn J.* 2021;13(6):1347-54. doi: 10.5530/pj.2021.13.170.
- Duong VA, Nguyen TT, Maeng HJ. Preparation of solid lipid nanoparticles and nanostructured lipid carriers for drug delivery and the effects of preparation parameters of solvent injection method. *Molecules.* 2020;25(20):1-36. doi: 10.3390/molecules25204781, PMID 33081021.
- Zhao Y, Chang YX, Hu X, Liu CY, Quan LH, Liao YH. Solid lipid nanoparticles for sustained pulmonary delivery of Yuxingcao essential oil: preparation, characterization and *in vivo* evaluation. *Int J Pharm.* 2017;516(1-2):364-71. doi: 10.1016/j.ijpharm.2016.11.046, PMID 27884712.
- Ebrahimi HA, Javadzadeh Y, Hamidi M, Jalali MB. Repaglinide-loaded solid lipid nanoparticles: effect of using different surfactants/stabilizers on physicochemical properties of nanoparticles. *Daru.* 2015;23(1):46. doi: 10.1186/s40199-015-0128-3, PMID 26392174.
- Lamidi S, Olaleye N, Bankole Y, Obalola A, Aribike E, Adigun I. Applications of response surface methodology (RSM) in product design, development and process optimization. In: Kayaroganam P, editor. *Response surface methodology-research and applications.* IntechOpen; 2023. doi: 10.5772/intechopen.106763.

15. Kumar R, Reji M. Response surface methodology (RSM): an overview to analyze multivariate data. *Indian J Microbiol Res.* 2023;9(4):241-8. doi: 10.18231/ijmr.2022.042.
16. Parmar VK, Desai SB, Vaja T. RP-HPLC and UV spectrophotometric methods for estimation of pirfenidone in pharmaceutical formulations. *Indian J Pharm Sci.* 2014;76(3):225-9. PMID 25035534.
17. Hasyati US, Surini S, Suhariyono GS. Prospective pulmonary drug delivery system of pirfenidone microparticles for pulmonary fibrosis. *J Appl Pharm Sci.* 2023;09:95-105. doi: 10.7324/JAPS.2023.125985.
18. Surini S, Providya R, Putri KS. Formula optimization of rifampicin dry powder inhalation with chitosan-xanthan carrier using response surface methodology. *J Appl Pharm Sci.* 2019;9(1):33-41. doi: 10.7324/JAPS.2019.90106.
19. Abdo RW, Saadi N, Hijazi NI, Suleiman YA. Quality control and testing evaluation of pharmaceutical aerosols. In: *Drug delivery systems.* Netherland. Elsevier; 2019. p. 579-614.
20. Maboos M, Yousuf RI, Shoaib MH, Nasiri I, Hussain T, Ahmed HF. Effect of lipid and cellulose based matrix former on the release of highly soluble drug from extruded/spheronized, sintered and compacted pellets. *Lipids Health Dis.* 2018;17(1):136. doi: 10.1186/s12944-018-0783-8, PMID 29885655.
21. Kumar JA, Bhikshapathi DV. Development of nilotinib loaded solid lipid nanoparticles and optimization by central composite design approach. *Int J App Pharm.* 2022;14(2):172-80. doi: 10.22159/ijap.2022v14i2.43943.
22. Farsani PA, Mahjub R, Mohammadi M, Oliaei SS, Mahboobian MM. Development of perphenazine-loaded solid lipid nanoparticles: statistical optimization and cytotoxicity studies. *BioMed Res Int.* 2021;2021:(6619195). doi: 10.1155/2021/6619195, PMID 33997026.
23. He Y, Guo F. Micromechanical analysis on the compaction of tetrahedral particles. *Chem Eng Res Des.* 2018;136:610-9. doi: 10.1016/j.cherd.2018.06.019.
24. Putri KS, Ramadhani LS, Rachel T, Suhariyono G, Surini S. Promising chitosan-alginate combination for rifampicin dry powder inhaler to target active and latent tuberculosis. *J Appl Pharm Sci.* 2022;12(5):98-103.
25. Chaurasiya B, Zhao YY. Dry powder for pulmonary delivery: a comprehensive review. *Pharmaceutics.* 2020;13(1):1-28. doi: 10.3390/pharmaceutics13010031, PMID 33379136.
26. Hirota K, Hasegawa T, Nakajima T, Inagawa H, Kohchi C, Soma GI. Delivery of rifampicin-PLGA microspheres into alveolar macrophages is promising for treatment of tuberculosis. *J Control Release.* 2010;142(3):339-46. doi: 10.1016/j.jconrel.2009.11.020, PMID 19951729.
27. Labiris NR, Dolovich MB. Pulmonary drug delivery. Part II: the role of inhalant delivery devices and drug formulations in therapeutic effectiveness of aerosolized medications. *Br J Clin Pharmacol.* 2003;56(6):600-12. doi: 10.1046/j.1365-2125.2003.01893.x, PMID 14616419.
28. Dudhat K, Patel H. Preparation and evaluation of pirfenidone loaded chitosan nanoparticles pulmonary delivery for idiopathic pulmonary fibrosis. *Futur J PharmSci.* 2022;8(1):1-14.
29. Ahmad I, Pandit J, Sultana Y, Mishra AK, Hazari PP, Aqil M. Optimization by design of etoposide loaded solid lipid nanoparticles for ocular delivery: characterization, pharmacokinetic and deposition study. *Mater Sci Eng C Mater Biol Appl.* 2019;100:959-70. doi: 10.1016/j.msec.2019.03.060, PMID 30948132.
30. Parvathaneni V, Kulkarni NS, Shukla SK, Farrales PT, Kunda NK, Muth A. Systematic development and optimization of inhalable pirfenidone liposomes for non-small cell lung cancer treatment. *Pharmaceutics.* 2020;12(3). doi: 10.3390/pharmaceutics12030206, PMID 32121070.
31. Rastogi V, Yadav P, Husain A, Verma A. Effect of hydrophilic and hydrophobic polymers on permeation of S-amlodipine besylate through intercalated polymeric transdermal matrix: 3(2) designing, optimization and characterization. *Drug Dev Ind Pharm.* 2019;45(4):669-82. doi: 10.1080/03639045.2019.1569035, PMID 30633579.
32. Aulia S, Winarti L, Wicaksono Y. Meloxicam self-nanoemulsifying drug delivery system: formulation and release kinetics analysis. *Int J App Pharm.* 2021;13Special Issue 4:188-93. doi: 10.22159/ijap.2021.v13s4.43856.
33. Hu L, Kong D, Hu Q, Gao N, Pang S. Evaluation of high-performance curcumin nanocrystals for pulmonary drug delivery both *in vitro* and *in vivo*. *Nanoscale Res Lett.* 2015;10(1):381. doi: 10.1186/s11671-015-1085-y, PMID 26428016.